

Density Functional Study of Metallacumulene Complexes

Nazzareno Re

Facoltà di Farmacia, Università G. D'Annunzio, I-66100 Chieti, Italy

Antonio Sgamellotti*

Dipartimento di Chimica e Centro Studi CNR per il Calcolo Intensivo in Scienze Molecolari, Università di Perugia, I-06123 Perugia, Italy

Carlo Floriani

Institut de Chimie Minérale et Analytique, Université de Lausanne, CH-1015 Lausanne, Switzerland

Received October 18, 1999

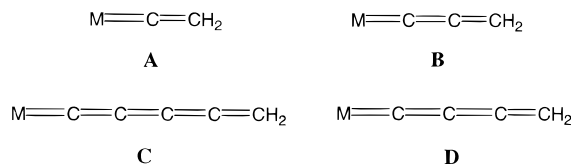
Density functional calculations have been carried out on the series of metallacumulene complexes $[(\text{CO})_5\text{Cr}(\text{=C})_n\text{H}_2]$ ($n = 2\text{--}9$) to study the electronic structure and the bonding of the C_nH_2 cumulene carbene moieties to d^6 transition metal fragments. Optimized geometries have been calculated for all complexes and found in good agreement with the available X-ray experimental data. The electronic structure has been analyzed in terms of the synergistic σ donation π back-donation model, and the contribution from π back-donation was found to be slightly higher than that from σ donation. Dissociation energies have been calculated for the metal–cumulene bond and have been found essentially independent of chain length. The perturbational theory of reactivity has been employed to explain the reactivity patterns of this class of complexes.

1. Introduction

Organometallic compounds containing a carbon-rich conjugating chain have recently received much interest. Several complexes of the type $[\text{L}_n\text{M}(\text{C})_n\text{ML}_n]$ are known in which two metal transition atoms are connected by linear carbon chains of up to 20 carbon atoms.^{1–4}

By contrast mononuclear $[\text{L}_n\text{M}(\text{=C})_n\text{H}_2]$ complexes with more than three carbon atoms are very rare and are only beginning to be studied.^{5–9} These compounds are known as metallacumulenes and constitute a new class of extended π -conjugated systems. After metal-lavinylidene complexes (**A** in Scheme 1), metal allenylidenes (**B**) are the simplest metallacumulenes. The first allenylidene metal complexes were synthesized in

Scheme 1



1976,^{10,11} and since then a variety of allenylidene derivatives have been prepared.^{12,13}

Recently, very few pentatetraenylidene metal complexes (**C**) have been synthesized and fully characterized.^{5,6} Complexes with $n > 5$ thus far have not been isolated or spectroscopically characterized. A butatrienylidene⁸ (**D**) and a heptahexaenylidene⁹ species have been suggested as plausible intermediates in the synthesis of some functionalized allenylidenes but not isolated.

These metallacumulene compounds attract attention for their material properties (especially liquid crystalline and nonlinear optical properties) and for their potential use as precursors to access metal-containing copolymers. Moreover, the presence of an $\text{M}=\text{C}$ bond and an unsaturated carbon chain offers potential applications in organometallic and organic synthesis.

(1) Beck, W.; Niemer, B.; Wieser, M. *Angew. Chem., Int. Ed. Engl.* **1993**, *32*, 923, and references therein.

(2) Lang, H. *Angew. Chem., Int. Ed. Engl.* **1994**, *34*, 547, and references therein.

(3) Zhou, Y.; Seyler, J. W.; Weng, W.; Arif, A. M.; Gladysz, J. A. *J. Am. Chem. Soc.* **1993**, *115*, 8509. Bartik, T.; Bartik, B.; Brady, M.; Dembinsky, R.; Gladysz, J. A. *Angew. Chem., Int. Ed. Engl.* **1996**, *35*, 414.

(4) Coat, F.; Guillevis, M.-A.; Toupet, L.; Paul, F.; Lapinte, C. *Organometallics* **1997**, *16*, 5988.

(5) Touchard, D.; Haquette, P.; Daridor, A.; Toupet, L.; Dixneuf, P. *H. J. Am. Chem. Soc.* **1994**, *116*, 11157. Peron, D.; Romero, A.; Dixneuf, P. *H. Gazz. Chim. Ital.* **1994**, *124*, 497. Peron, D.; Romero, A.; Dixneuf, P. *H. Organometallics* **1995**, *14*, 3319.

(6) Lass, R. W.; Steinert, P.; Wolf, J.; Werner, H. *Chem. Eur. J.* **1996**, *2*, 19.

(7) Roth, G.; Fisher, H. *Organometallics* **1996**, *15*, 1139.

(8) Bruce, M. I.; Hinterding, P.; Low, P. J.; Skelton, B. W.; White, A. W. *J. Chem. Soc., Chem. Commun.* **1996**, 1009. Lompfrey, J. R.; Selegue, J. P. *Organometallics* **1993**, *12*, 616.

(9) Roth, G.; Fisher, H. *Organometallics* **1996**, *15*, 5766.

(10) Fisher, E. O.; Kalder, H. J.; Frank, A.; Köhler, F. H.; Huttner, G. *Angew. Chem., Int. Ed. Engl.* **1976**, *15*, 623.

(11) Berke, H. *Angew. Chem., Int. Ed. Engl.* **1976**, *15*, 624.

(12) Antonova, A. B.; Ioganson, A. A. *Russ. Chem. Rev. (Engl. Transl.)* **1989**, *58*, 693. Doherty, S.; Corrigan, J. F.; Carty, A. J.; Sappa, E. *Adv. Organomet. Chem.* **1995**, *37*, 39.

(13) Bruce, M. I.; Swincer, A. G. *Adv. Organomet. Chem.* **1983**, *22*, 59. Bruce, M. I. *Chem. Rev.* **1991**, *91*, 197.

Geometric and spectroscopic features of this class of compounds suggest that cumulene carbene ligands are strong π donors.^{12,14} The observed M–C and C–C bond lengths indicate substantial π contribution for the metal–carbon bond and, on average, double carbon–carbon bond, while the infrared spectra are consistent with reduced $\nu(\text{C}\equiv\text{C})$ stretching frequencies. Simple considerations suggest that the d_π to π^* back-donation should be high.

The cumulene carbene ligand, $(\text{C}=\text{C})_n\text{CH}_2$, is susceptible to both electrophilic and nucleophilic attack, allowing for further transformations and functionalization. Considerable knowledge has been achieved in the chemistry and the reactivity of vinylidene and allenylidene metal complexes.^{12,13} Metal vinylidenes are highly reactive and susceptible to nucleophilic attack at the C_1 carbon and electrophilic attack at the C_2 carbon, while metal allenylidenes undergo nucleophilic attack on the C_1 or C_3 carbons, respectively, by hard or soft nucleophiles, and electrophilic attack at the C_2 carbon.

On the other hand, little is known on the reactivity of metal pentatetraenylidene complexes. The few available data give evidence for regioselective nucleophilic attack at the C_1 or C_3 and electrophilic attack at the C_1 .^{5,6}

To our knowledge a few theoretical investigations have been performed only on the simplest metallacumulene complexes^{15–19}—vinylidene and allenylidene species—and essentially at the semiempirical level.^{16–19} Extended Hückel calculations have been reported on related polymers.²⁰

In this paper we have performed LCAO density functional calculations on a series of $[(\text{CO})_5\text{Cr}(\text{C}=\text{C})_n\text{H}_2]$ ($n = 2–9$) complexes, as models of metallacumulene up to nonaoctaenylidene metal species.

The $[(\text{CO})_5\text{Cr}]$ metal fragment has been used as representative of d^6 $\text{Cr}(0)$, $\text{Mo}(0)$, and $\text{W}(0)$ metal systems, which are quite common in the chemistry of metal allenylidenes and vinylidenes^{12,13} and of Fischer-type transition metal carbenes.²¹ This fragment is also implied, together with $[(\text{CO})_5\text{W}]$, in two diheteroatom-substituted pentatetraenylidene metal complexes recently synthesized.⁷

We have carried out geometry optimizations and studied the stability of these complexes, the nature of π conjugation along the metal and carbon atoms, and their dependence on the chain length.

We have also made use of the perturbational theory of reactivity, examining the charge distribution, the energies, and localization properties of the frontier orbitals, to explain the known reactivity patterns of this

class of complexes and to study their variation on increasing the chain length. This analysis gave a rationale for the regioselectivity for electrophilic and nucleophilic attack in terms of both charge distribution and localization of the frontier orbitals along the carbon atoms of the cumulene chain.

2. Computational Details

The calculations reported in this paper are based on the ADF (Amsterdam Density Functional) program package.²² Its main characteristics are the use of a density fitting procedure to obtain accurate Coulomb and exchange potentials in each SCF cycle, the accurate and efficient numerical integration of the effective one-electron Hamiltonian matrix elements, and the possibility to freeze core orbitals. The molecular orbitals were expanded in an uncontracted triple- ζ Slater-type orbitals (STO) basis set for all main group atoms. For Cr orbitals we used a double- ζ STO basis set for 3s and 3p and a triple- ζ STO basis set for 3d and 4s. As polarization functions, we used one 4p function for Cr, one 3d for C and O, and one 2p for H. The inner shell cores have been kept frozen.

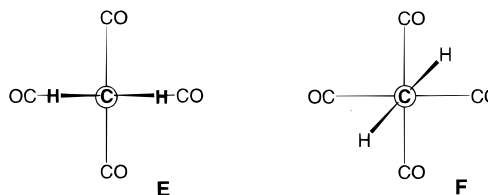
The LDA exchange correlation potential and energy were used, together with the Vosko–Wilk–Nusair parametrization²³ for homogeneous electron gas correlation, including the Becke's nonlocal correction^{24a} to the local exchange expression and the Perdew's nonlocal correction^{24b} to the local expression of correlation energy. Molecular structures of all considered complexes were optimized at this nonlocal (NL) level in C_{2v} symmetry.

The coordinate system has been chosen so that the z axis is in the Cr–C(chain) direction and the cumulene plane lies in the xz plane.

3. Results and Discussion

Geometry Optimization. There can be two different conformations of the $[(\text{CO})_5\text{Cr}(\text{C}=\text{C})_n\text{H}_2]$ complexes with the C_nH_2 plane arranged eclipsed or staggered with the cis carbonyl ligands (**E** and **F** in Scheme 2). Preliminary

Scheme 2



calculations on the vinylidene complex gave the two conformations very close in energy (ca. 1 kJ mol^{–1}), indicating an essentially free rotation around the M–C bond. We therefore considered only eclipsed conformations, which allow a simpler bonding analysis.

All the considered complexes have been optimized and showed a $^1\text{A}_1$ singlet ground state. The optimized parameters concerning the metal fragment are reported in Table 1, while those concerning the cumulene unit are illustrated in Figure 1. The geometries of even-chain cumulenes are consistent with a purely cumulenic structure, the C–C bond lengths ranging from 1.27 to

(14) Bruce, M. I. *Coord. Chem. Rev.* **1997**, 166, 91. Touchard, D.; Dixneuf, P. H. *Coord. Chem. Rev.* **1998**, 178, 409.

(15) Ehlers, A. W.; Dapprich, S.; Vyboishchikov, S. F.; Frenking, G. *Organometallics* **1996**, 15, 105.

(16) Schilling, B. E. R.; Hoffmann, R.; Lichtenberger, D. L. *J. Am. Chem. Soc.* **1979**, 101, 585. Schilling, B. E. R.; Hoffmann, R.; Faller, J. W. *J. Am. Chem. Soc.* **1979**, 101, 592.

(17) Kostić, N. M.; Fenske, R. F. *Organometallics* **1982**, 1, 974.

(18) Esteruelas, M. A.; Gómez, A. V.; López, A. M.; Modrego, J.; Oñate, E. *Organometallics* **1997**, 16, 5826.

(19) Berke, H.; Huttner, G.; von Seyer, J. Z. *Naturforsch., B: Anorg. Chem., Org. Chem.* **1981**, 36B, 1277.

(20) Frapper, G.; Kertesz, M. *Inorg. Chem.* **1993**, 32, 732. Re, N.; Sgamellotti, A.; Floriani, R. *J. Chem. Soc., Dalton Trans.* **1998**, 2521.

(21) Dötz, K. H.; Fisher, H.; Hofmann, P.; Kreissl, F. R.; Shubert, U.; Weiss, K. *Transition Metal Carbene Complexes*; VCH Publishers: Weinheim, Germany, 1983.

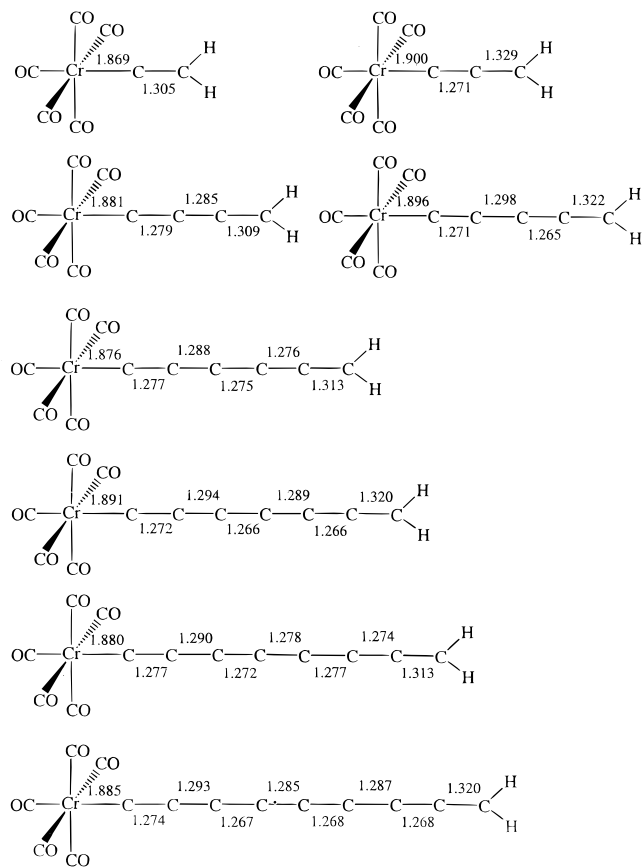
(22) Baerends, E. J.; Ellis, D. E.; Ros, P. *Chem. Phys.* **1973**, 2, 42. Boerrigter, P. M.; te Velde, G.; Baerends, E. J. *Int. J. Quantum Chem.* **1988**, 33, 87.

(23) Vosko, S. H.; Wilk, L.; Nusair, M. *Can. J. Phys.* **1980**, 58, 1200.

(24) (a) Becke, A. D. *Phys. Rev. A* **1988**, 38, 2398. (b) Perdew, J. P. *Phys. Rev. B* **1986**, 33, 8822.

Table 1. Optimized Geometrical Parameters Concerning the Metal Fragments in $(\text{CO})_5\text{Cr}(\text{=C})_n\text{H}_2$ Complexes^a

	$n = 2$	$n = 3$	$n = 4$	$n = 5$	$n = 6$	$n = 7$	$n = 8$	$n = 9$
$\text{R}(\text{Cr}-\text{CO})_{\text{ax}}$	1.948	1.939	1.938	1.939	1.942	1.941	1.946	1.944
$\text{R}(\text{Cr}-\text{CO})_{\text{eqII}}$	1.921	1.918	1.932	1.917	1.932	1.918	1.929	1.918
$\text{R}(\text{Cr}-\text{CO})_{\text{eq}\perp}$	1.912	1.932	1.923	1.930	1.923	1.930	1.920	1.929
$\text{R}(\text{C}-\text{O})_{\text{ax}}$	1.153	1.154	1.153	1.154	1.153	1.153	1.152	1.152
$\text{R}(\text{C}-\text{O})_{\text{eqII}}$	1.153	1.154	1.151	1.153	1.151	1.153	1.151	1.152
$\text{R}(\text{C}-\text{O})_{\text{eq}\perp}$	1.154	1.151	1.152	1.151	1.152	1.151	1.152	1.151
$\text{R}(\text{C}-\text{Cr}-\text{C}_{\text{eqII}})$	89.5	86.8	88.9	87.4	88.6	87.3	88.5	87.7
$\text{R}(\text{C}-\text{Cr}-\text{C}_{\text{eq}\perp})$	86.3	89.0	87.4	88.4	87.7	88.4	87.9	88.7

^a Bond lengths in angstroms and bond angles in degrees.**Figure 1.** Optimized parameters concerning the cumulene unit in $(\text{CO})_5\text{Cr}(\text{=C})_n\text{H}_2$ complexes. Bond lengths in angstroms and bond angles in degrees.

1.29 Å, except for the terminal C-C bond, which is markedly longer, 1.32–1.34 Å, as expected for sp^2 hybridization of the terminal carbon atoms. The geometries of odd-chain cumulenes show a small but significant polyene-like carbon-carbon bond length alternation superimposed to an average cumulenic structure. Two slightly different types of C-C bond lengths are observed, falling in the ranges 1.26–1.27 and 1.29–1.33 Å. The short Cr-C distance, in the range 1.87–1.90 Å, is typical of a chromium-carbon double bond.²¹

A direct comparison between theoretical and experimental geometries is difficult, as most of the observed structures refer to aryl- or alkyl-substituted cumulenes and different metal fragments. In particular, the experimental data in Table 2 refer to a few allenylidene^{19,25,26} and one pentatetraenylidene⁵ complex with

Table 2. Experimental M-C and C-C Distances (Å) for Some Allenylidene and Pentatetraenylidene Complexes

molecule	M-C ₁	C ₁ -C ₂	C ₂ -C ₃	C ₃ -C ₄	C ₄ -C ₅
$(\text{CO})_5\text{Cr}(\text{=C})_3\text{R}^{25}$	1.913(7)	1.26(1)	1.359(9)		
$\text{Cp}(\text{CO})_2\text{Mn}(\text{=C})_3\text{Cy}_2^{19}$	1.806(6)	1.252(8)	1.342(8)		
$\text{Cp}(\text{Pme}_3)_2\text{Ru}(\text{=C})_3\text{Ph}_2^{26}$	1.884(5)	1.255(8)	1.329(9)		
$\text{Cl}(\text{dppe})_5\text{Ru}(\text{=C})_5\text{Ph}_2^{+5}$	1.891(9)	1.25(1)	1.30(1)	1.24(1)	1.36(1)

Table 3. Optimized Geometries of the C_nH_2 Cumulenes^a

n	C ₁ -C ₂	C ₂ -C ₃	C ₃ -C ₄	C ₄ -C ₅	C ₅ -C ₆	C ₆ -C ₇	C ₇ -C ₈	C ₈ -C ₉
2	1.289							
3	1.293	1.327						
4	1.291	1.291	1.302					
5	1.291	1.301	1.265	1.321				
6	1.291	1.294	1.271	1.279	1.307			
7	1.292	1.297	1.266	1.289	1.266	1.319		
8	1.292	1.295	1.268	1.282	1.275	1.276	1.310	
9	1.292	1.297	1.297	1.286	1.267	1.288	1.267	1.319

^a Only C-C bond lengths (angstroms) are reported.

d⁶ metal fragments. The calculated values show a qualitative agreement with the above experimental data. In particular, for the only allenylidene complex with a $\text{Cr}(\text{CO})_5$ fragment Cr-C and C-C bond length deviations are within only 0.04 Å and could, in part, be due to the use of hydrogen substituents on the terminal carbon atom instead of the real substituents.

It is also worth comparing the geometries of the C_nH_2 units in the considered complexes with those for the corresponding free cumulene carbenes to point out their distortion upon coordination. These C_nH_2 molecules have been proposed by radioastronomy to be constituents in interstellar gas, and those with $n = 3$ and 4 have been spectroscopically identified.²⁷ A few ab initio calculations have been recently performed on the ground and the lowest excited states of cumulene carbenes to support astrophysical measurements.²⁸ In ref 28b extensive calculation have been performed on carbenes up to $n = 15$, showing a closed shell ground state for all molecules, and optimized geometries have been calculated for both the ground and a few lowest excited states. We performed NL-DFT calculations on the singlet ground states of these cumulene carbenes fragments up to $n = 9$. The results of our calculation are reported in Table 3 and are in good agreement with those of ref 28b obtained at the MP2 level with a 6-31G** basis set.

A comparison between the C-C bond lengths of the $[(\text{CO})_5\text{Cr}(\text{=C})_n\text{H}_2]$ complexes (Figure 1) and those of the

(25) Berke, H.; Härter, P.; Huttner, G.; von Seyerl, J. *J. Organomet. Chem.* **1981**, 219, 317.

(26) Selegue, J. P. *Organometallics* **1982**, 1, 217.

(27) Thaddeus, P.; Gottlieb, C. A.; Mollaghababa, R.; Vrtilek, J. M. *Chem. Phys.* **1993**, 89, 2125.

(28) (a) Maluendes, S. A.; McLean, A. D. *Chem. Phys. Lett.* **1992**, 200, 511. (b) Fischer, G.; Maier, J. P. *Chem. Phys.* **1997**, 223, 149.

corresponding free cumulene carbenes (Table 3) shows a significant distortion of these unsaturated ligands upon coordination, probably due to the population of the two lowest unoccupied orbitals (see below).

Electronic Structure. The electronic structure of these $[(\text{CO})_5\text{Cr}(\text{=C})_n\text{H}_2]$ complexes is discussed by a fragment approach in which the C_nH_2 unit interacts with the $[(\text{CO})_5\text{Cr}]$ metal fragment.

The $[(\text{CO})_5\text{Cr}]$ fragment has a pseudo-octahedral geometry with one ligand removed and presents an approximate C_{4v} symmetry. The frontier d orbitals are constituted by a lower set of three t_{2g} -like orbitals, labeled as $1a_2(d_{xy})$, $1b_1(d_{xz})$, and $1b_2(d_{yz})$ in the C_{2v} point group, slightly mixed with the π^* orbitals of the CO ligands, and by two higher e_g -like orbitals, labeled as $1a_1(d_z, p_z \text{ hybrid})$ and $2a_1(d_{x^2-y^2})$; see Figures 2 or 3 on the left. The $2a_1$ is of δ symmetry and lies at high energies due to the interactions with the equatorial CO 5σ . The other d_δ orbital, $1a_2$, is significantly stabilized by the back-bonding to the equatorial CO π^* . The two d_π orbitals, b_1 and b_2 , are almost degenerate and are stabilized by the back-bonding to the axial and two of the equatorial CO π^* .

The cumulene carbene C_nH_2 fragments all have closed shell 1A_1 ground states with a lone pair of electrons on the initial C_1 carbon atom. This lone pair corresponds to a high lying doubly occupied orbital of a_1 symmetry, which is the HOMO for C_2H_2 and the HOMO-1 for all other considered cumulenes.

With the end CH_2 group defining a plane, the π system of the C_nH_2 carbenes is made up by a set of n out-of-plane π orbitals (hereafter called π_\perp , all of b_1 symmetry) and a set of $n - 1$ in-plane π orbitals (hereafter called π_\parallel , all of b_2 symmetry), occupied by $2n - 2$ electrons. As a consequence, these molecules divide into two series, n odd and n even. Molecules with n odd present a HOMO of π_\parallel character and a LUMO of π_\perp character, while molecules with n even have a π_\perp HOMO and a π_\parallel LUMO (Figure 4). The main π accepting properties of these unsaturated ligands are determined by the LUMO and, to a lesser extent, by the LUMO+1. Upon chain lengthening, the HOMO–LUMO gap decreases from 3.1 eV for C_2H_2 to 1.05 eV for C_9H_2 . In particular the LUMO shows a strong energy lowering (from -4.3 to -6.3 eV), which would suggest an increase of the π acceptor properties with chain length.

Figures 2 and 3 illustrate the orbital interaction diagram for $[(\text{CO})_5\text{Cr}(\text{=C})_4\text{H}_2]$ and $[(\text{CO})_5\text{Cr}(\text{=C})_5\text{H}_2]$, which are representative of the behavior of metallacumulenes with n even and n odd, respectively.

There are three main orbital interactions between the $[(\text{CO})_5\text{Cr}]$ metal fragment and the C_4H_2 or C_5H_2 moiety. (i) The cumulene σ orbital donates into the metal d_z , forming the metal–carbon σ bond. (ii) One of the two filled quasi-degenerate d_π metal orbitals back-donates into the empty LUMO of the cumulene unit (b_2 for C_4 or b_1 for C_5). (iii) The remaining filled d_π orbital interacts with both the filled HOMO and the empty LUMO+1 of cumulene (b_1 for C_4 or b_2 for C_5); the former corresponds to a destabilizing filled–filled (two-orbital four-electron) interaction, while the latter gives a minor stabilizing π back-donation contribution.

Two different π back-bonding interactions, occurring in two orthogonal planes, can therefore be distin-

E (eV)

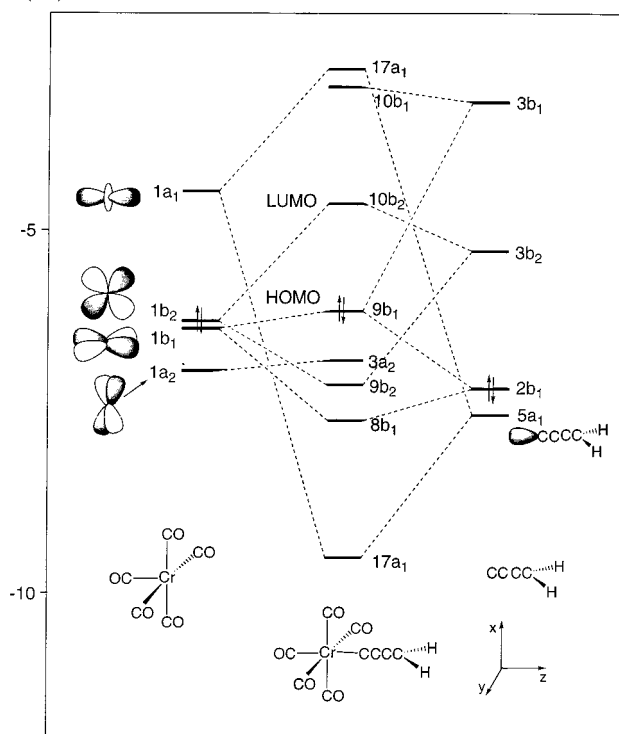


Figure 2. Orbital interaction diagram for $(\text{CO})_5\text{Cr}(\text{=C})_4\text{H}_2$.

E (eV)

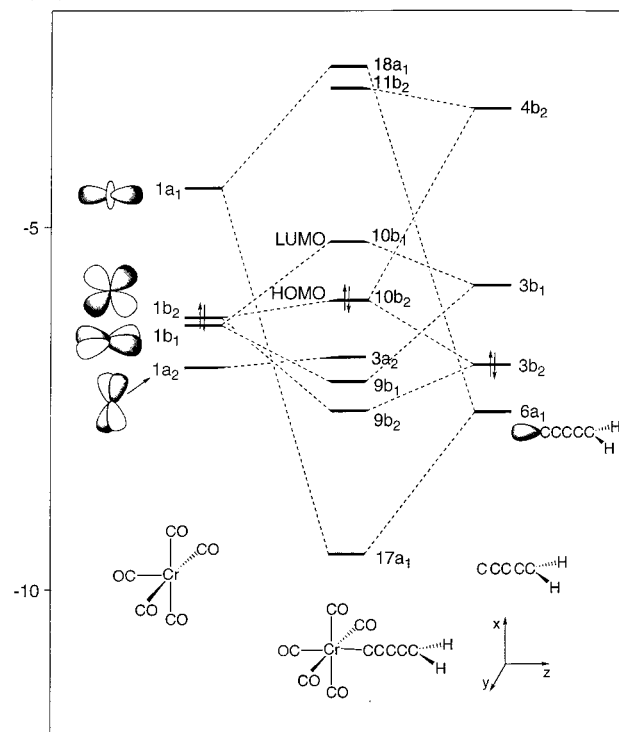


Figure 3. Orbital interaction diagram for $(\text{CO})_5\text{Cr}(\text{=C})_5\text{H}_2$.

guished: a major contribution coming from the LUMO (π_\parallel for C_4 or π_\perp for C_5) and a minor contribution from the LUMO+1 (π_\perp for C_4 or π_\parallel for C_5).

On lengthening the cumulene chain from C_2 to C_9 , the HOMO–LUMO gap decreases (compare, for instance, Figures 2 and 3), in agreement with the UV/vis spectra of $[(\text{CO})_5\text{Cr}(\text{=C})_n(\text{NR}_2)_2]$ ($n = 3, 5$), which show a bathochromic shift from C_3 to C_5 .⁷

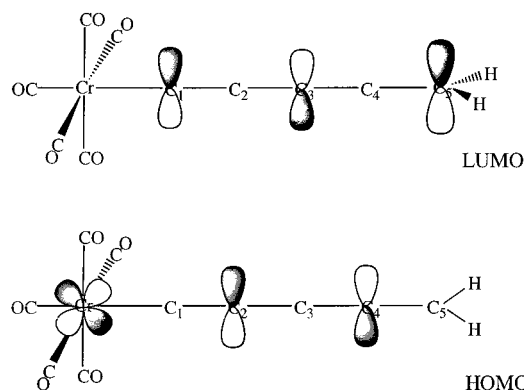
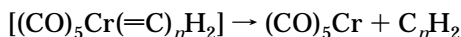


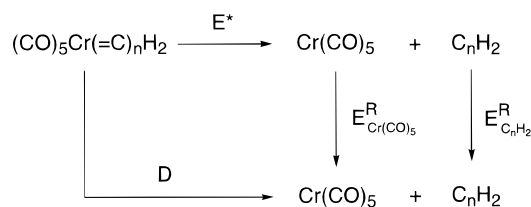
Figure 4. Sketch of the orbital composition of HOMO and LUMO for $(\text{CO})_5\text{Cr}(=\text{C})_n\text{H}_2$.

Bonding Energies. The bond dissociation energies between the $\text{Cr}(\text{CO})_5$ and C_nH_2 fragments, $D(\text{Cr}-\text{C}_n\text{H}_2)$, have been calculated according to the following scheme:



where both the cumulene complex and the two fragments have been considered in their ground-state equilibrium geometries. Using the fragment-oriented approach of the DFT computational scheme implemented in the ADF program, the above bond dissociation energies are computed in two steps, as shown in Scheme 3. First we calculate the “snapping energies”, $E^*(\text{Cr}-$

Scheme 3



C_nH_2), i.e., the energies gained when snapping the metal–cumulene bond, obtained by building $[(\text{CO})_5\text{Cr}(=\text{C})_n\text{H}_2]$ from the fragments with the conformation they assume in the equilibrium geometry of the overall complex. In a second step we compute the energies $E^{\text{R}}_{\text{C}_n\text{H}_2}$ and $E^{\text{R}}_{(\text{CO})_5\text{Cr}}$ gained when the isolated fragments relax to their equilibrium geometries. Corrections for the zero-point vibrations were not included since they are expected to be quite small. Indeed, the vibrational zero-point corrections to metal–ligand bonding energy have been calculated to be ca. 4–18 kJ mol^{-1} ²⁹ for $(\text{CO})_5\text{W}=\text{CR}_2$ carbene complexes and are expected to be smaller for chromium complexes and longer chains. A recent investigation of the effects of the basis set incompleteness on the bond dissociation energies of some metal–ligand and metal–metal bonds has led to the conclusion that triple- ζ plus polarization basis sets give reasonably accurate bond energies for organometallic systems with sufficiently small BSSE corrections to warrant its neglect in most situations.³⁰

The results obtained are given in Table 4, where we report both contributions, i.e., snapping energies and

Table 4. Calculated Bond Dissociation Energies for the $(\text{CO})_5\text{Cr}(=\text{C})_n\text{H}_2$ Complexes (kJ mol^{-1})

n	E^*	$E^{\text{R}}_{\text{Cr}(\text{CO})_5}$	$E^{\text{R}}_{\text{C}_n\text{H}_2}$	D_e
2	282	13	1	268
3	294	9	2	283
4	286	9	1	276
5	294	10	2	282
6	286	10	1	275
7	292	10	2	280
8	270	10	1	259
9	290	10	2	278

relaxation energies, and show relatively high bonding energies (270–285 kJ mol^{-1}). A comparison with experimental data is not possible since, to the best of our knowledge, no bonding energy has been measured for vinylidene or higher cumulene complexes. However, the theoretically predicted high bond energy for $(\text{CO})_5\text{CrC}_2\text{H}_2$ is supported by the experimentally observed high thermodynamic stability of vinylidene complexes.^{12,13} It is noteworthy that the bonding energy calculated for $(\text{CO})_5\text{CrC}_2\text{H}_2$, 268 kJ mol^{-1} , compares quite well with the value of 279 kJ mol^{-1} calculated by Frenking and co-workers at an accurate CCSD(T)/MP2 level.¹⁵

Table 4 also shows that the chromium–cumulene bond dissociation energies remain almost constant on lengthening the cumulene chain, showing only a very little decrease. This suggests that there is no thermodynamic upper limit to the cumulene chain length, the synthetic difficulties to prepare metallacumulene with carbon chains longer than three carbon atoms being probably connected with the high reactivity of these species.

Bonding Analysis. The bonding of an unsaturated σ, π ligand coordinated to a transition metal fragment is usually described by a synergistic σ donation π back-donation, i.e., the Dewar–Chatt–Duncanson model.³¹ According to this model, the bonding arises from the electron donation from a filled σ orbital of the ligand to a suitable vacant metal orbital (σ donation) and the simultaneous back-donation from occupied metal d orbitals to the low-lying vacant π^* orbitals of the ligand (π back-donation). The considered $(\text{CO})_5\text{Cr}$ metal fragment shows a LUMO of a_1 symmetry with hybrid $s-p_z$ character and two filled b_1 and b_2 orbitals of d_π character; see Figure 2. The σ donation involves essentially the empty metal a_1 orbital and the filled a_1 orbital describing the lone pair on the initial carbon atom of C_nH_2 . The π back-donation involves the filled $b_1(d_{xz})$, $b_2(d_{yz})$ metal orbitals and the two lowest empty π^* orbitals of C_nH_2 of b_1 and b_2 symmetry. For odd n the LUMO is of b_1 symmetry and is responsible for most of the accepting properties of the organic fragment, while the LUMO+1 is of b_2 symmetry and, being higher in energy, shows minor accepting properties; see Figure 3. For even n the LUMO is b_2 , while the LUMO+1 is of b_1 symmetry; see Figure 2.

To separate the contributions from σ donation and π back-donation, we employed an analysis of the metal–olefins bond dissociation energies based on the extended transition state method.^{32a} The bond dissociation energy is decomposed into a number of contributions:

(31) Dewar, M. J. S. *Bull. Soc. Chim. Fr.* **1951**, 18, C71. Chatt, J.; Duncanson, L. A. *J. Chem. Soc.* **1953**, 2939.

(32) (a) Ziegler T.; Rauk, A. *Theor. Chim. Acta* **1977**, 46, 1. (b) Ziegler, T. *NATO ASI* **1986**, C176, 189.

(29) Vyboishchikov, S. F.; Frenking, G. *Chem. Eur. J.* **1998**, 4, 1428.

(30) Rosa, A.; Ehlers, A. W.; Baerends, E. J.; Snijders, J. G.; te Velde, G. *J. Phys. Chem.* **1996**, 100, 5690.

$$D(\text{Cr}-\text{C}_n\text{H}_2) = -[E_{\text{prep}} + E_{\text{ster}} + E_{\text{orb}}]$$

The first term, E_{prep} , is the energy necessary to convert the fragments from their equilibrium geometries to the conformation they assume in the optimized structure of the overall complex and, eventually, the promotion energy from the ground to the valence states. Since the valence states of the $(\text{CO})_5\text{Cr}$ and C_nH_2 fragments are the same closed shell ground states they show as free molecules, this term corresponds simply to the sum of the fragments' relaxation energies, $E_{\text{C}_n\text{H}_2}^{\text{R}} + E_{\text{Cr}(\text{CO})_5}^{\text{R}}$. E_{ster} represents the steric repulsion between the two fragments and consists of two components. The first component is the electrostatic interaction of the nuclear charges and the unmodified electronic charge density of one fragment with those of the other fragment. The second component is the so-called Pauli repulsion, which is essentially due to the four-electron destabilizing interactions between occupied orbitals. E_{orb} , known as the orbital interaction term, represents the attracting orbital interactions which give rise to the energy lowering upon coordination. This term may be broken up into contributions from the orbital interactions within the various irreducible representations Γ of the overall symmetry group of the system, according to the decomposition scheme proposed by Ziegler.^{32b}

This decomposition scheme is particularly useful in the considered complexes, as it allows one to separate the energy contributions corresponding to σ donation (E_{A1}) and to π back-donation ($E_{\text{B1}} + E_{\text{B2}}$). Indeed, the ligand-to-metal donation takes place into the A_1 representation, while the metal-to-ligand back-donation takes place into the B_1 and B_2 representations. In particular for odd n E_{B1} represents the energy contribution from the back-donation into the LUMO (b_1) and E_{B2} the contribution from back-donation into the LUMO+1 (b_2), while for even n the symmetries of the two contributions are exchanged.

Indeed, although the orbital interaction energy in b_1 and b_2 symmetry is in principle the sum of forward- and back-bonding components, for a Cr^0 (d^6) ion the d_π subset is fully occupied and the overlap with the filled C_nH_2 HOMO constitutes the destabilizing four-electron two-orbital repulsion whose energetic contribution is found in E_{ster} .

The results of this energy decomposition for all the considered olefin complexes are reported in Table 5. It follows from Table 5 that the overall contribution to the orbital interaction term from π back-donation, $E_{\text{B1}} + E_{\text{B2}}$, is slightly higher than that from σ donation, E_{A1} .

It is worth noting that a recent CDA analysis of metal–vinylidene donor–acceptor interactions in $(\text{CO})_5\text{CrC}_2\text{H}_2$, investigated at the MP2 level, showed that vinylidene is a slightly better σ donor than π acceptor in terms of charge transfer.¹⁵ Therefore our results show that metal-to-vinylidene π back-donation, although implying a minor charge transfer, is energetically more important than vinylidene-to-metal σ donation. This difference between charge-transfer and energetic donation/back-donation strength has been observed for other σ -donating π -accepting ligands such as CO ¹⁵ and olefins.³³

(33) Nunzi, F.; Re, N.; Sgamellotti, A.; Floriani, R. *J. Chem. Soc., Dalton Trans.* **1999**, 3487.

Table 5. Bond Dissociation Energy Decomposition for the $(\text{CO})_5\text{Cr}(\text{=C})_n\text{H}_2$ Complexes (kJ mol^{-1})

n	E_{ster}	E_{orb}	E_{A1}	E_{A2}	E_{B1}	E_{B2}	$E_{\text{B1}} + E_{\text{B2}}$
2	145	−427	−203	0	−65	−160	−225
3	113	−407	−197	0	−157	−54	−211
4	130	−415	−196	0	−75	−147	−222
5	116	−410	−196	0	−148	−68	−216
6	137	−423	−197	0	−86	−145	−231
7	122	−414	−197	0	−145	−77	−222
8	150	−421	−196	0	−90	−140	−230
9	125	−418	−197	0	−143	−85	−228

Table 5 also shows that on lengthening the cumulene chain the σ contribution (E_{A1}) and the π contribution ($E_{\text{B1}} + E_{\text{B2}}$) remain essentially constant. This seems, at first sight, quite surprising since upon chain lengthening the LUMO of the C_nH_2 cumulene carbenes shows a strong energy lowering (see above), which would suggest an increase of their π -accepting properties. However, the energy lowering of the LUMO is counterbalanced by its enhanced delocalization over a longer chain, leading to a lesser effective overlap with the $\text{d}_\pi(\text{Cr})$. This is confirmed by an analysis of the $\text{LUMO}(\text{C}_n\text{H}_2) - \text{d}_\pi(\text{Cr})$ overlap integral, which decreases from a value of 0.167 for C_2H_2 to 0.074 for C_9H_2 .

Reactivity. Besides geometry and the electronic structure of these compounds, we have studied their reactivity and regioselectivity toward nucleophilic and electrophilic additions.

The cumulene carbene ligand, C_nH_2 , may undergo both electrophilic and nucleophilic attack, allowing for further transformations and functionalization. Metal vinylidenes are highly reactive and susceptible to nucleophilic attack at the C_1 carbon and electrophilic attack at the C_2 carbon, while metal allenylidenes undergo nucleophilic attack at the C_1 or C_3 carbons and electrophilic attack at the C_2 carbon.^{12,13}

On the other hand, little is known about the reactivity of higher metallacumulenes. The few available data for metal pentatetraenylidenes give evidence for regioselective nucleophilic attack at the C_1 or C_3 and electrophilic attack at the C_2 .^{5,6} The chemistry of butatrienylidenes⁸ and heptahexaenylidenes,⁹ never isolated but only hypothesized as intermediates in the synthesis of some functionalized allenylidenes and pentatetraenylidenes, has been interpreted in terms of nucleophilic attack at the C_3 and C_5 and electrophilic attack at C_4 .

Our analysis follows the approach of Fukui,³⁴ further generalized by Klopman,³⁵ which distinguish between charge-controlled chemical reactions, where the regioselectivity is determined by the charge distribution, and frontier-controlled reactions, where regioselectivity is determined by the frontier orbital localization.

The reactivity and regioselectivity of carbene, vinylidene, and allenylidene metal complexes has already been theoretically addressed through Fenske–Hall and extended Hückel calculations.^{17–19} The regioselectivity toward electrophiles was interpreted in terms of charge and orbital factors in concert, while the regioselectivity

(34) Fukui, K.; Yonezawa, T.; Nagata, C. *J. Chem. Phys.* **1957**, *27*, 1247. Fukui, K.; Yonezawa, T.; Nagata, C. *J. Chem. Phys.* **1959**, *31*, 550. Fukui, K. *Theory of Orientation and Stereoselection*; Springer: Berlin, 1975.

(35) Klopman, G.; Hudson, R. F. *Teor. Chim. Acta* **1967**, *8*, 1965. Klopman, G. *J. Am. Chem. Soc.* **1968**, *90*, 223. Klopman, G. In *Chemical Reactivity and Reaction Paths*; Klopman, G., Ed.; Wiley: New York, 1974; pp 59–67.

Table 6. Mulliken Charges on the Metal and Chain Carbon Atoms (CO)₅Cr(=C)_nH₂ Complexes

<i>n</i>	Cr	C ₁	C ₂	C ₃	C ₄	C ₅	C ₆	C ₇	C ₈	C ₉
2	+0.60	−0.09	−0.34							
3	+0.53	−0.15	+0.06	−0.18						
4	+0.52	−0.15	+0.06	+0.09	−0.19					
5	+0.52	−0.14	+0.01	+0.06	+0.03	−0.13				
6	+0.53	−0.14	−0.02	+0.01	+0.01	+0.07	−0.18			
7	+0.53	−0.14	−0.01	+0.01	−0.04	+0.04	+0.04	−0.13		
8	+0.54	−0.13	−0.01	+0.01	−0.05	+0.01	+0.02	+0.08	−0.16	
9	+0.54	−0.13	−0.01	+0.01	−0.03	−0.01	−0.03	+0.03	+0.05	−0.13

Table 7. Breakdowns of the Orbital Contributions from the Metal and Cumulene Carbon Atoms for the HOMO and LUMO of (CO)₅Cr(=C)_nH₂ Complexes

<i>n</i>	orbital	Cr	C ₁	C ₂	C ₃	C ₄	C ₅	C ₆	C ₇	C ₈	C ₉
2	HOMO	49.7	3.3	22.0							
	LUMO	12.5	58.2	2.0							
3	HOMO	47.2	5.8	20.1	0.8						
	LUMO	30.4	15.0	4.0	35.7						
4	HOMO	38.6	4.6	16.5	1.8	18.8					
	LUMO	12.8	33.1	3.6	32.6	1.2					
5	HOMO	37.2	6.4	16.3	2.7	15.5	0.1				
	LUMO	13.8	20.1	7.2	20.1	3.2	26.6				
6	HOMO	30.8	5.2	14.1	1.4	13.8	1.3	16.5			
	LUMO	11.9	22.3	4.5	22.6	1.8	23.3	0.1			
7	HOMO	30.6	6.3	14.0	2.2	13.3	2.0	12.9	0.1		
	LUMO	12.5	15.1	5.0	14.3	3.6	16.7	2.0	21.3		
8	HOMO	25.9	5.3	12.1	1.8	11.6	0.9	12.0	1.0	14.4	
	LUMO	11.0	16.8	4.7	16.6	2.3	18.2	1.3	18.0	0.1	
9	HOMO	25.5	6.1	12.1	2.4	11.6	1.5	11.4	1.6	11.1	0.1
	LUMO	11.3	12.1	5.5	11.0	2.9	12.7	1.5	14.3	1.5	17.8

toward nucleophilic attack was attributed to the localization of the LUMO orbitals.

For all the considered cumulene metal complexes we performed a Mulliken population analysis calculating the gross atomic charges on the metal, the carbonyls, and the various carbon atoms of the cumulene ligand. The results are reported in Table 6 and clearly show that charge distribution is not important in determining the regioselectivity of both electrophilic and nucleophilic attack.

Indeed, Table 6 shows no significant charge differences among the various carbon atoms of the cumulene chains; all carbon atoms bear very small positive or negative charges without any apparent trend except for significantly higher negative charges on the first and last carbon atoms.

Only for the vinylidene complex does the Mulliken analysis show a significant polarization of the charge distribution on the carbon atoms of the unsaturated ligand, with the C₂ bearing a higher negative charge than C₁, and suggests that the regioselectivity of the electrophilic attack could be explained by charge factors in agreement with the Fenske–Hall analysis of ref 18.

The molecular orbital diagrams of the C₄ and C₅ metallacumulenes in Figures 2 and 3 show a high-lying HOMO and a low-lying LUMO, suggesting that the high reactivity of these complexes toward both electrophilic and nucleophilic attack is determined by frontier orbital factors. Moreover, since the HOMO is quite isolated in energy from the other highest occupied MOs (by ca. 0.8 eV in C₄ and 0.9 eV in C₅) and the LUMO is even better isolated from the other lowest unoccupied orbitals (by ca. 1.6 eV in C₄ and 1.9 eV in C₅), these two orbitals play the main role in determining the regioselectivity of, respectively, the electrophilic and nucleophilic attack.

The breakdowns of the contribution from the metal and the carbon atoms along the chain to the HOMO and LUMO of all [(CO)₅Cr(=C)_nH₂] cumulenes are listed in Table 7 and show a quite peculiar pattern.

For all considered complexes the HOMO (b₂ for odd *n* or b₁ for even *n*) has contributions mainly from the metal and the carbon atoms in even positions along the chain, i.e., C₂, C₄, C₆, etc., while the LUMO (b₁ for odd *n* or b₂ for even *n*) has contributions mainly from the carbon atoms in odd positions along the chain, i.e., C₁, C₃, C₅, etc.

The localization of the LUMO at the carbon atoms in odd positions of the cumulene chains (C₁, C₃, C₅, ...) causes the nucleophilic attack to be regioselective on these atoms, in agreement with the known reactivity patterns of vinylidene,^{12,13} allenylidene,^{12,13} and pentatetraenylidene complexes,^{5,6} and those hypothesized for the butatrienylidene⁸ and heptahexaenylidene⁹ intermediates.

At the same time, the localization of the HOMO at the carbon atoms in even positions (C₂, C₄, C₆, ...) determines the regioselectivity of an electrophilic attack to these atoms, still in agreement with the experimental evidence.^{5–9,12,13}

It is noteworthy that on increasing the chain length there is an energy increase of the HOMO and a lowering of the LUMO, which determines an increase of the reactivity toward both electrophilic and electrophilic attack and is probably the reason for the synthetic difficulties in preparing higher metallacumulenes.

These results not only reproduce very well the known reactivity patterns for the lower metallacumulene complexes but also allow one to foresee the regioselectivity of the higher cumulenes, whose synthesis and characterization have recently attracted much interest.

4. Conclusions

Density functional calculations have been carried out on the series of metallacumulene complexes $[(\text{CO})_5\text{Cr}-(=\text{C})_n\text{H}_2]$ ($n = 2-9$) to study the electronic structure and the bonding of the C_nH_2 cumulene carbene moieties to d^6 transition metal fragments. Optimized geometries have been calculated for all complexes and found in good agreement with the available X-ray experimental data. The electronic structure has been analyzed in terms of the synergistic σ donation π back-donation model, and the contribution from π back-donation was found to be slightly higher than that from σ donation. Dissociation energies have been calculated for the metal–cumulene bond and have been found essentially independent of chain length, suggesting that there is no thermodynamic upper limit to the cumulene chain length and that the synthetic difficulties to prepare metallacumulenes with carbon chains longer than three carbon atoms are due only to the high reactivity of these species.

The perturbational theory of reactivity has been employed to explain the reactivity patterns of this class of complexes and has shown that the regioselectivity of both electrophilic and nucleophilic attack is frontier orbital controlled. We have found that the LUMO is mainly localized on the odd carbon atoms (C_1 , C_3 , C_5 , ...), thus determining their electrophilic character. On the other hand, the HOMO is localized on the even carbon atoms (C_2 , C_4 , C_6 , ...), thus determining their nucleophilic character.

Acknowledgment. The present work has been carried out in the context of the COST D9 Action. Thanks are due to the CNR (Progetto Finalizzato “Materiali Speciali per Tecnologie Avanzate II”) for financial support.

OM990824T